Atmospheric Environment 193 (2018) 79–87

Contents lists available at ScienceDirect

Atmospheric Environment

journal homepage: www.elsevier.com/locate/atmosenv

Projecting the impacts of atmospheric conditions under climate change on air quality over the Pearl River Delta region

Cheuk Hei Marcus Tong[a], Steve Hung Lam Yim[a,b,c,*], Daniel Rothenberg[d], Chien Wang[d], Chuan-Yao Lin[e], Yongqin David Chen[f,a,b], Ngar Cheung Lau[a,b]

[a] Department of Geography and Resource Management, The Chinese University of Hong Kong, Hong Kong, China
[b] Institute of Environment, Energy and Sustainability, The Chinese University of Hong Kong, Hong Kong, China
[c] Stanley Ho Big Data Decision Analytics Research Centre, The Chinese University of Hong Kong, Hong Kong, China
[d] Center for Global Change Science, Massachusetts Institute of Technology, Cambridge, MA, USA
[e] Research Center for Environmental Changes, Academia Sinica, Taipei, Taiwan
[f] School of Humanities and Social Science, The Chinese University of Hong Kong, Shenzhen, Hong Kong, China

ARTICLE INFO

Keywords:
Air quality
Climate change
Trans-boundary air pollution
Generalized linear models
General circulation model

ABSTRACT

Anthropogenic climate change has been increasingly confirmed by weather observation and scientific literature in recent decades. Atmospheric stability, which has strong effects on vertical mixing of air pollutants and thus air quality, may be affected under climate change. This study aims to statistically assess the impacts of climate change alone on the future air quality in the Pearl River Delta region in the near future (2030–2039) and the far future (2090–2099) under two Representative Concentration Pathways (RCP) scenarios, i.e., RCP 4.5 and RCP 8.5, based on the future surface and upper level meteorological data projected by one regional climate model (RCM): WRF, and by four general circulation models (GCMs): CanESM2, MIROC, MRI-CGCM3 and MPI-ESM-LR. The arithmetic means of projections reveal an increase in the levels of air pollutants [ozone (O_3), respirable suspended particulates (RSP) and sulphur dioxide (SO_2)] in various seasons, even though a decrease is projected to occur in June-July-August. These changes in projected mean concentration are more significant in the far future, and under the RCP8.5 scenario. Among difference meteorological variables, surface temperature is most associated with the projected change in the three pollutants, with a range from 56.9% to 65.2% in all seasons and for all pollutants, relative to all contributions in RCP8.5 for example. Other notable associations include positive effects of vertical temperature gradient and the temperature–dew point difference on pollutant concentration. We found an increase in frequency of high pollution levels in December–January–February and March–April–May, as the occurrence proportion of pollutant concentration greater than the recent 95th percentile is 9.5%–9.6% and 6.4%–9.2%, respectively. We conclude that climate change alone is projected to have significant effect on air quality in the Pearl River Delta region in future, implying the necessity of more stringent air pollutant emission control policies to mitigate air pollution in the future.

1. Introduction

Air pollution is strongly influenced by weather conditions, and is therefore sensitive to climate change. The Intergovernmental Panel on Climate Change (IPCC) projected that air quality in cities will be degrading in the future (IPCC, 2014), with some studies attributing the effect to increase in anticyclonic conditions (e.g. Hulme and Jenkins, 2002). Particularly, many previous studies have adopted air quality models to investigate the influence of climate change on the increase in O_3 concentrations (Morris et al., 1989, 1995; Penner et al., 1989; Sillman and Samson, 1995; Sillman, 1999). Particularly, Dawson et al. (2007) and Hedegaard et al. (2008) suggested that temperature is one of the greatest contributors among the meteorological parameters. Some studies have also highlighted that both the increases in temperature and radiation contribute the most to projected O_3 increase in the 21st century (Krüger et al., 2008). On the other hand, changes in circulation patterns at synoptic and global scales due to climate change can also affect pollution levels (e.g., Collins et al., 2003; Stevenson et al., 2006). Most previous studies have focused on the projection of O_3 concentration only, whereas a few studies have highlighted the role of wet deposition on the removal of particulate matters and SO_2 through increased precipitation (e.g. Tagaris et al., 2007). Yet, projecting air

* Corresponding author. Department of Geography and Resource Management, The Chinese University of Hong Kong, Hong Kong, China.
E-mail address: steveyim@cuhk.edu.hk (S.H.L. Yim).

https://doi.org/10.1016/j.atmosenv.2018.08.053
Received 30 April 2018; Received in revised form 27 August 2018; Accepted 28 August 2018
Available online 29 August 2018
1352-2310/ © 2018 Elsevier Ltd. All rights reserved.

quality for future years is challenging because of its complex nature. Air quality is influenced by different factors that often interfere one another that masking effects make the understanding to processes and contribution of each factor separately difficult.

Furthermore, the impacts of climate change on air quality vary from region to region due to the change of the pollutant emission patterns (Fiore et al., 2012), and the differential meteorological pattern in terms of synoptic, mesoscale, and turbulent scale (Pielkea et al., 1998). Most of these outcomes mentioned were obtained in Europe or in the US. Yet, studies focusing on the Asia and Pacific region where regional monsoons determine seasonal meteorological variability are insufficient (IPCC, 2014). The Pearl River Delta (PRD) region has been accommodating tens of millions of inhabitants in major urban areas. The rapid urbanization and economic development in the PRD have contributed to complex regional air pollution problems associated with rising anthropogenic emissions (Wang et al., 2003; Wu et al., 2005; Zhang et al., 2008a). In addition to global scale climate change, notable effects of urbanization have also contributed to the regional climate change in the PRD. Wang et al. (2014) has found a rise of surface temperature, but a drop of surface absolute humidity and wind speed in the PRD in recent years, which is pointed to the reduction in vegetation and irrigated cropland. Projections by Liu et al. (2013) have suggested a climate change induced increase in afternoon mean surface O_3 by 1.5 ppb from 2000 to 2050. Studies have been focused mostly on O_3 which is associated with various chemical interactions in the atmosphere. A clear and comprehensive study on the sign and magnitude of climate change impacts on air quality in the PRD region still requires further investigations.

We note that previous studies have projected future air quality based on surface meteorological factors alone. Yet, vertical atmospheric stability, which is often defined by various meteorological factors such as temperature, humidity and wind speed along the vertical profile (e.g. George, 1960; Miller, 1967; Shir and Shieh, 1974), has played an important role on mixing pollutants emitted from different sources (Lo et al., 2006), as well as allowing accumulation and chemical reaction of pollutants under stagnant airflow conditions (Wu et al., 2005). Previous studies have run general circulation model (GCM) or regional climate model (RCM) simulations to study climate change's effect on mixing depth for the 21st century, but both increases and decreases of mixing depths are found in different regions without consistent patterns (Hogrefe et al., 2004; Mickley et al., 2004; Leung and Gustafson, 2005; Murazaki and Hess, 2006; Lin et al., 2008; Wu et al., 2008). Notable model uncertainty has also implied that the projected trends are not robust (Murazaki and Hess, 2006). Moreover, none of these studies have applied meteorological variables measured at different altitudes to project the role of climate change on the vertical transport of air pollutants and hence the air quality.

Above all, our aim of this study is to project the sole effects of climate change on future air quality with various GCM & RCM meteorological data based on linear models, and to evaluate the contribution of each of these meteorological variables on the future projection.

2. Data and methods

2.1. Site selection

The PRD region has been selected as the focus of this study. This area is a large flatland surrounded by the Nanling Mountains which isolate the air pollution in the PRD from that in central China (Zhang et al., 2008b). Nonetheless, the arrival of the northeast monsoon during winter period sometimes transports pollutants from eastern and northern China along the coastline to the PRD region (Yim et al., 2010; Gu and Yim, 2016). Under stagnant airflow conditions, the basin-shaped PRD limits pollutant dispersion. Some local-scale meteorological patterns like urban heat islands, land–sea breezes, and mountain–valley winds are associated with mixing and re-circulating air pollutants emitted from different places within the PRD region (Lo et al., 2006). The topographic and meteorological features have combined altered the processes of pollutant accumulation and reaction (Wu et al., 2005; Yim et al., 2007) in terms of various spatial scales (local, PRD regional or beyond the PRD region) depending on the specific synoptic conditions (Huang et al., 2005Wang et al., 2009).

The PRD, which is consisted of nine major cities and two special administrative regions – Hong Kong and Macao, has contributed approximately 70% of the gross domestic product (GDP) in Guangdong Province (Wang et al., 2014). Rapid urbanization is witnessed in the PRD over the past few decades, with a 72.7% of the total land has been designated as urban land use as of 2010 (Wang et al., 2014). Besides, the absolute population has multiplied from 24.0 million in 1990 to 56.1 million in 2014. Serious air pollution associated with massive urbanization and industrialization remains to be a critical problem in the region. Local emissions are contributed by the intensive industrial activities and facilities which produce intensive pollutant emissions in various categories (Zheng et al., 2009). While both the fraction of urbanized land and region population are projected to continue to increase in the future, the pollution problem is projected to remain significant in the next decades.

2.2. GLM models for air quality projections

The projection models adopted in this study are derived by Tong et al. (2018). They developed generalized linear models (GLM) which correlate the meteorological variables along altitudes with the surface air quality at several selected measuring stations in the PRD. The predictor meteorological variables in the model, derived by the basic meteorological parameters of classical stability indices like K-index (George, 1960) and Bulk Richardson Number (Baklanov et al., 2002; Borge et al., 2008; Shir and Shieh, 1974), includes temperature at surface level, and vertical temperature difference, temperature–dew point difference, north-south and east-west wind components along four vertical levels up to 700 mb, approximately 3000 m where anthropologic aerosol typically exists below this level (see Table 1). Regarding the response of air quality variables, our study focuses on the projection of ozone (O_3), respirable suspended particulates (RSP) and sulphur dioxide (SO_2). These pollutants are considered as major air pollutants in the PRD region, and produced from both local and non-local emission sources (Che et al., 2011; Luo et al., 2018; Wang and Lu, 2006). They are usually adopted as indicators to assess the ambient air quality in the PRD such as the Air Quality Health Index due to their adverse impacts on human health and plants (Wong et al., 2013). These pollutants can be potentially transported over long distances (Fiore et al., 2009), thus their ambient concentrations can be significantly altered by variability in atmospheric conditions.

2.3. Future meteorological projection data

The future meteorological data are simulated by a monthly ensemble of various GCMs & RCM [hereafter referred to as climate models]. The climate models include MPI-ESM-LR (Giorgetta et al., 2013), MRI-CGCM3 (Yukimoto et al., 2012), MIROC5 (Watanabe et al.,

Table 1
Meteorological variables used in the study.

Temperature (°C)	2 m **(T_{2m})**
Temperature Difference (°C)	2 m–925 mb **(T_{2m})**, 925 mb–850 mb **($T_{925\text{-}850}$)**, 850 mb–700 mb **($T_{850\text{-}700}$)**
Temperature–Dew Point Difference (°C)	2 m **($T\text{-}D_{2m}$)**, 925 mb **($T\text{-}D_{925}$)**, 850 mb **($T\text{-}D_{850}$)**, 700 mb **($T\text{-}D_{700}$)**
U wind component (m/s)	10 m **(U_{10m})**, 925 mb **(U_{925})**, 850 mb **(U_{850})**, 700 mb **(U_{700})**
V wind component (m/s)	10 m **(V_{10m})**, 925 mb **(V_{925})**, 850 mb **(V_{850})**, 700 mb **(V_{700})**

2010), CanESM2 (Chylek et al., 2011) and WRF (Lin et al., 2015). These models have been well evaluated and chosen depending on the availability of the meteorological variables required in the study (Jiang et al., 2016). Considering the model uncertainty, the minimum, mean and maximum values of each sample month are picked among the projected values from these models, so as to create the minimum, mean and maximum distribution projections in the future. The meteorological conditions under the near future (2030–2039, NF) and the far future (2090–2099, FF) under the Representative Concentration Pathways (RCP) 4.5 and 8.5 scenarios are studied.

2.4. Statistical models

We apply the future meteorological projection data to the GLMs for climate projection. The GCM performance has been comprehensively documented in previous studies: WRF (Lin et al., 2015), MPI-ESM-LR (Giorgetta et al., 2013), MRI-CGCM3 (Yukimoto et al., 2012), MIROC5 (Watanabe et al., 2010), and CanESM2 (Chylek et al., 2011). For the performance of our GLM, an intensive model evaluation was conducted in our previous study (Tong et al., 2018). To further validate the application, we adopt the 1994–2003 and 2015–2016 climate model data and compare the simulated air quality data with ground observation data in these years, provided by Hong Kong Environment Protection Department. Generally, they show notable agreements with each other after standardization, as the refined indices of agreement (Willmott et al., 2012) are 0.62, 0.71, 0.53 for O_3, RSP and SO_2 in 1994–2003 and 0.53 (0.52), 0.60 (0.62) and 0.49 (0.47), for those under the 2015–2016 climate model RCP 4.5 (RCP 8.5) data.

The future projection of air quality is based on the following equation:

$$P_j(k) = \sum_{i=1}^{N} [z_i(k) \times S_{ij}]$$

where $P_j(k)$ is the projected pollutant j concentration in the sample k. $z_i(k)$ is the future deviation of the meteorological variable i in the sample k. S_{ij} *is the* regression coefficient vector between meteorological variable i and pollutant j. The products are summed up with a total of N meteorological variables. These variables are standardized by the recent observation values in 1994–2003. These projected samples are then combined to form air quality distributions, based on different time and scenarios.

We examine the role of each meteorological variable on the future air quality projection by its future contribution, which is defined by the change in the meteorological variable and the power of the coefficients of the meteorological variable:

$$C_{ij}(k) = z_i(k) \times S_{ij} \times \mu_j$$

where $C_{ij}(k)$ is the contribution of meteorological variable i on the pollutant j in the sample k. $z_i(k)$ is the future deviation of the meteorological variable i in the sample k, standardized by the recent climate model data set. S_{ij} is the regression coefficient vector between meteorological variable i and pollutant j. μ_j is the climate model recent mean of pollutant j. All samples of the contribution values with the same projection decade and scenario are averaged to derive the results.

3. Results and discussion

3.1. Projected future changes of the meteorological variables

We evaluate the future change in meteorological variables projected by climate models taking into account the combined effects of global climate change, as well as the regional contributions due to urbanization effects. The future deviations of the mean distribution of the meteorological variables are demonstrated in Table 2, with the significant changes greater than 95% confidence level highlighted. The most notable change is the consistent projected increase in surface temperature in all seasons, consistent with previous studies (Wang et al., 2014) and projections (Ginn et al., 2010; Lee et al., 2011). In the near future, significant increases ($p < 0.005$) in T_{2m} are also found in DJF (0.90–0.96) and JJA (0.73–0.88), and the difference is not significant between the two RCP scenarios. In the far future, the projected increases in T_{2m} are found to be significant in all seasons of both scenarios, ranging from 1.52 to 1.77 K in RCP 4.5 ($p < 0.008$), and from 3.49 to 3.56 K in RCP 8.5 ($p < 0.001$) for the four seasons.

The projected increase of surface temperature in MAM is greater than that of the temperature at 925 mb, leading a projected rise of future temperature gradient between surface and upper levels. In the far future, the gradient is projected to increase significantly by 0.15–0.18 K. Yet, the temperature gradient is projected to decline at higher altitudes: Significant decreases in $T_{850\text{-}700}$ are found in the far future RCP 8.5 scenario (0.39–0.72 K) in MAM, JJA and SON ($p < 0.001$), as well as under the far future RCP 4.5 scenario (0.27–0.29 K) in MAM and JJA ($p < 0.003$).

The surface temperature–dew point difference is found to increase in the future, implying a decline of surface relative humidity in the future. This finding is consistent with the literature (Wang et al., 2014). The change is found statistically significant in the far future RCP 8.5 scenarios for all seasons, with a 0.35 K–0.56 K increase in $T–D_{2m}$ for the four seasons. The season with most notable changes in $T–D_{2m}$ is MAM, in which the projected increase is found statistically significant in most scenarios (NF RCP 4.5, FF RCP 4.5 and FF RCP 8.5; $p < 0.003$). Similar results ($p < 0.028$) are also observed at the 925 mb altitude for the scenarios of NF RCP 8.5, FF RCP 4.5 and FF RCP 8.5.

Despite some previous studies have revealed the change in wind flow due to the variation in synoptic circulation patterns and the modifications due to urbanization activities, the model projections do not show significant change in wind (U and V) in most situations. The only relatively notable change reductions occur in westerly wind at the 850 mb altitude and in southerly wind at the 700 mb altitude in the far future RCP 8.5 scenario in MAM, by 0.53 and 0.47 m/s, respectively.

3.2. Trend of air pollution in future climate scenarios

Fig. 1 shows the probability density function plots of the distributions including all monthly samples in the 10-year studied period, classified by pollutant species and scenarios. All distributions (blue lines) have shown a right shift from the recent (black lines) to future distributions, indicating an increase in pollutant concentration for all scenarios. Compared to the results of recent years, the mean percentage changes in O_3 in the near future and the far future under RCP 4.5 scenario are respectively 6.6% (actual change (ac): 2.8 μg/m^3; change range (cr): -4.9–11.1 μg/m^3) and 9.8% (ac: 4.1 μg/m^3; cr: -2.7–12.4 μg/m^3), being the greatest among the three pollutants. On the other hand, those under RCP 8.5 are 4.2% (ac: 1.8 μg/m^3; cr: -6.2–9.3 μg/m^3) and 14.0% (ac: 5.9 μg/m^3; cr: -5.3–17.4 μg/m^3), respectively.

Comparatively, for RSP, the mean changes under RCP 4.5 scenario are 4.3% (ac: 2.2 μg/m^3; cr: −19.5–21.9 μg/m^3) and 6.1% (ac: 13.54 μg/m^3; cr: −6.98–35.63 μg/m^3) in near future and far future. Those of RCP 8.5 are 4.6% (ac: 2.3 μg/m^3; cr: −16.8–19.3 μg/m^3) in near future, similar to the RCP 4.5 scenarios, but much greater increase (13.3%; ac: 6.8 μg/m^3; cr: −17.8–33.5 μg/m^3) is observed in far future.

While for SO_2, projected increases under RCP 4.5 in the near future and the far future are 4.2% (ac: 0.70 μg/m^3; cr: −4.46–5.95 μg/m^3) and 4.5% (ac: 1.05 μg/m^3; cr: −4.07–6.94 μg/m^3), showing that the increase is not significant between the near and the far future. Under RCP 8.5, percentage increase in the near future projection is 5.0% (ac: 0.8 μg/m^3; cr: −4.4–6.1 μg/m^3), similar to that of RCP 4.5, whereas that in the near future projection is 9.8% (ac: 1.5 μg/m^3; cr: −4.1–8.3 μg/m^3), comparatively larger than the projection under RCP 4.5 scenario.

After all, consistent increase is found (1) between recent and near

Table 2
Distribution changes of meteorological variables in different seasons and scenarios. Variables associated with temperature and temperature–dew point difference are presented in K, whereas variables associated with wind are presented in m/s. Significant changes with p-values smaller than 0.05 in two-sample T test are highlighted in yellow, and those smaller than 0.005 are highlighted in red. DJF refers to December-January-February; MAM refers to March-April-May; JJA refers to June-July-August; and SON refers to September-October-November.

		T_{2m}	T_{2m-925}	$T_{925-850}$	$T_{850-700}$	$T\text{-}D_{2m}$	$T\text{-}D_{925}$	$T\text{-}D_{850}$	$T\text{-}D_{700}$	U_{10m}	U_{925}	U_{850}	U_{700}	V_{10m}	V_{925}	V_{850}	V_{700}
MAM	NF45	0.97	0.13	0.11	-0.12	0.29	0.20	-0.06	0.09	-0.11	-0.15	-0.19	-0.20	0.16	0.17	0.03	-0.20
	NF85	0.99	0.00	0.05	-0.11	0.16	0.25	0.07	0.43	-0.02	0.04	-0.08	-0.23	0.07	0.04	-0.20	-0.19
	FF45	1.77	0.15	0.12	-0.27	0.36	0.26	-0.04	0.40	-0.10	-0.24	-0.49	-0.65	0.08	-0.06	-0.23	-0.21
	FF85	3.56	0.18	-0.03	-0.58	0.56	0.45	0.25	0.55	-0.16	-0.33	-0.53	-0.62	0.05	-0.03	-0.30	-0.47
JJA	NF45	0.73	0.00	-0.02	-0.13	0.01	-0.07	-0.15	-0.25	-0.16	-0.19	-0.07	0.06	0.04	0.17	0.20	0.09
	NF85	0.88	-0.03	0.02	-0.06	0.06	0.00	-0.16	-0.34	-0.10	-0.15	-0.13	-0.01	-0.14	-0.20	-0.24	-0.36
	FF45	1.52	0.07	0.00	-0.29	0.13	0.01	-0.14	-0.13	-0.14	-0.20	-0.31	-0.39	0.08	0.10	0.08	0.07
	FF85	3.54	0.07	-0.02	-0.39	0.37	0.21	-0.06	-0.29	-0.18	-0.16	-0.21	-0.38	0.13	0.29	0.06	-0.15
SON	NF45	0.97	0.02	-0.03	-0.09	0.04	0.01	-0.09	0.16	-0.07	0.03	0.20	-0.11	0.20	0.46	0.28	0.07
	NF85	0.97	0.04	-0.10	-0.11	0.16	0.12	0.13	0.16	-0.01	0.14	0.23	0.04	0.20	0.34	0.15	0.12
	FF45	1.66	0.06	-0.06	-0.22	0.15	0.06	-0.02	0.29	-0.04	0.02	0.01	-0.34	0.25	0.40	0.28	0.27
	FF85	3.53	0.04	-0.04	-0.72	0.35	0.09	-0.16	0.71	0.15	0.36	0.24	-0.38	0.34	0.43	0.14	0.24
DJF	NF45	0.96	0.02	0.02	-0.19	0.19	0.13	0.32	0.67	0.00	0.16	0.19	0.10	0.13	0.18	0.01	-0.06
	NF85	0.90	-0.03	-0.05	-0.11	0.11	0.13	0.35	0.21	-0.03	0.01	-0.10	-0.14	0.16	0.17	-0.02	-0.07
	FF45	1.64	-0.02	-0.06	-0.17	0.22	0.20	0.38	0.34	-0.06	-0.11	-0.22	-0.27	0.03	-0.07	-0.13	0.19
	FF85	3.49	-0.07	-0.10	-0.32	0.48	0.40	0.74	0.72	0.02	-0.03	-0.34	-0.78	0.27	0.15	-0.14	0.01

future, as well as (2) between near future to far future. The effect is projected to be more severe under the RCP 8.5 scenario in terms of distribution mean. Nonetheless, the model uncertainty range, indicated by the distribution of minimum values in green lines and the distribution of maximum values in pink lines, reveals a certain variation in our results driven by different climate models.

The distribution is classified into four seasons to observe whether there are noticeable changes in particular seasons. Table 3 demonstrates the projected change of the mean distribution for each season. The changes in particular seasons are relatively significant than the combined changes in the whole year. We highlight and conclude the significant seasonal percentage changes below.

DJF is highlighted because of the largest escalation from the recent mean among seasons. Projections under RCP 8.5 scenario in far future have the largest departure from the recent distribution, that there are projected 32.6%, 43.7% and 40.4% increase in O_3, RSP and SO_2, respectively. The projected means in the near future are around one-sixth to one-fourth of the projected mean in the far future, with a projected increase of 7.7%, 9.4% and 8.0% for O_3, RSP and SO_2, respectively. Considering RCP 4.5, the increases of pollutant concentration in the near (far) future are 11.0% (14.1%), 12.6% (18.4%) and 11.8% (15.7%) for O_3, RSP and SO_2, respectively, with only a slight elevation between the near and the far future values. MAM is also found to have a consistent increase in all future projections. O_3 has shown the greatest departure from the recent distribution, with projected increases of 11.8% (19.2%) and 7.6% (23.9%) in the near and the far future for RCP

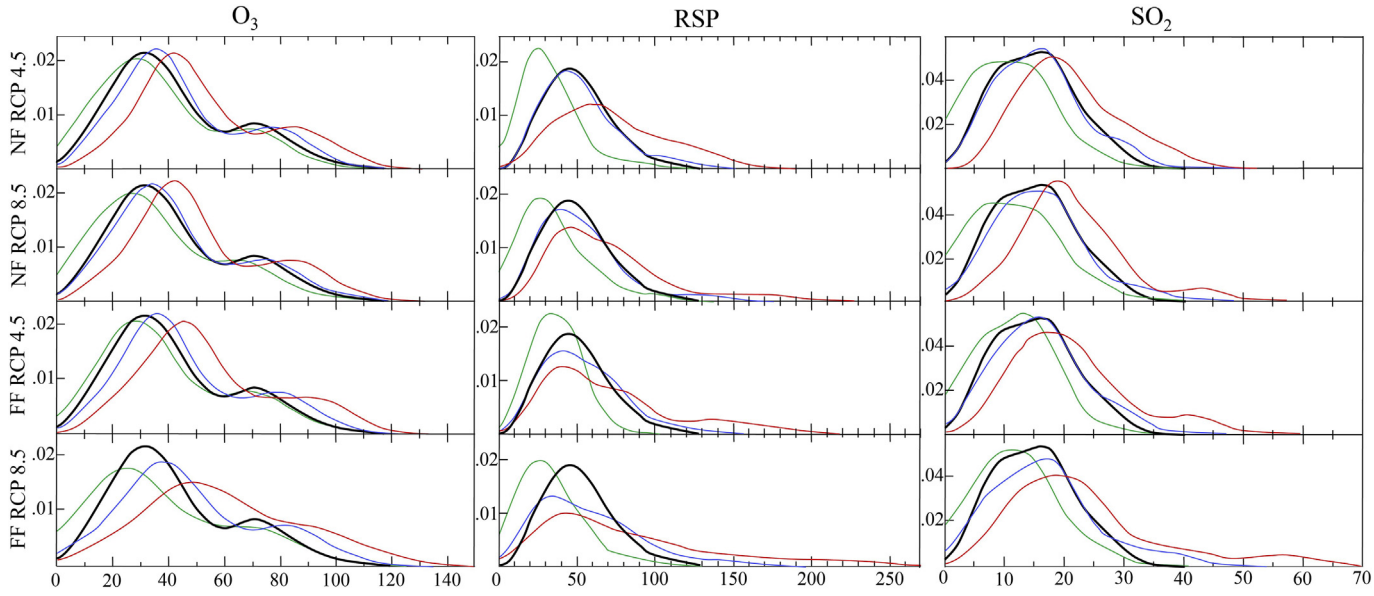

Fig. 1. Probability Density Function Plots of the projected distributions of O_3, RSP and SO_2 concentration (μg/m^3) averaged over the PRD region. The rows are in ascending order of Representative Concentration Pathways (RCP) 4.5 and 8.5 in near future (NF), and far future (FF). Black refers to the recent observation in 1994–2003; green refers to minimum projection; blue refers to mean projection; red refers to maximum projection. (For interpretation of the references to color in this figure legend, the reader is referred to the Web version of this article.)

Table 3
Distribution changes in air pollutant concentration in different seasons and scenarios. Model uncertainty is presented by the range of minimum and maximum values. Units of the recent means and the absolute changes in the pollutants are in μg/m^3. The mean percentage deviation from the recent mean is also highlighted. DJF refers to December–January–February; MAM refers to March–April–May; JJA refers to June–July–August; and SON refers to September–October–November.

	MAM						JJA					
	Recent Mean	Scenario	Changes				Recent Mean	Scenario	Changes			
			Min	Mean	Max	%			Min	Mean	Max	%
O_3	46.28	**NF4.5**	−1.2	5.5	15.1	**11.8%**	30.76	**NF4.5**	−3.8	−0.3	3.9	**−1.1%**
		NF8.5	−5.2	3.5	11.2	**7.6%**		**NF8.5**	−4.7	−1.4	2.3	**−4.4%**
		FF4.5	0.1	8.9	21.4	**19.2%**		**FF4.5**	−5.7	−1.4	4.0	**−4.6%**
		FF8.5	5.6	11.1	18.3	**23.9%**		**FF8.5**	−17.3	−6.7	0.2	**−21.7%**
RSP	47.36	**NF4.5**	−11	0.9	14.1	**1.9%**	28.17	**NF4.5**	−5.2	0.1	7.1	**0.4%**
		NF8.5	−11.9	0.6	11.8	**1.2%**		**NF8.5**	−6.6	1.1	9.1	**3.8%**
		FF4.5	−4.7	2.2	10.3	**4.5%**		**FF4.5**	−4.2	−0.3	4.7	**−1.0%**
		FF8.5	−4.1	1.9	10.0	**4.1%**		**FF8.5**	−8.6	−2.9	4.4	**−10.3%**
SO_2	13.08	**NF4.5**	−2.1	0.8	4.0	**6.0%**	12.67	**NF4.5**	−5.8	−0.1	5.5	**−0.8%**
		NF8.5	−2.6	0.5	3.6	**4.0%**		**NF8.5**	−5.8	0.8	8.8	**6.0%**
		FF4.5	−0.5	1.6	4.1	**12.2%**		**FF4.5**	−5.4	−0.6	3.9	**−4.4%**
		FF8.5	0.6	2.0	4.2	**15.2%**		**FF8.5**	−7.5	−2.8	4.0	**−22.4%**
	SON						**DJF**					
	Recent Mean	Scenario	Changes				Recent Mean	Scenario	Changes			
			Min	Mean	Max	%			Min	Mean	Max	%
O_3	51.08	**NF4.5**	−9.3	1.8	11.8	**3.6%**	40.07	**NF4.5**	−5.0	4.4	14.1	**11.0%**
		NF8.5	−6.5	1.9	8.9	**3.8%**		**NF8.5**	−8.4	3.1	15.1	**7.7%**
		FF4.5	−1.0	3.7	7.7	**7.2%**		**FF4.5**	−4.3	5.7	17.2	**14.1%**
		FF8.5	−5.8	6.6	20.8	**13.0%**		**FF8.5**	−3.0	13.1	30.8	**32.6%**
RSP	58.70	**NF4.5**	−22.8	−0.8	18.7	**−1.3%**	69.35	**NF4.5**	−39.6	8.7	48.8	**12.6%**
		NF8.5	−13.8	1.3	10.5	**2.2%**		**NF8.5**	−35.6	6.5	47.3	**9.4%**
		FF4.5	−14.2	−1.7	10.4	**−2.9%**		**FF4.5**	−31.9	12.7	59.2	**18.4%**
		FF8.5	−29.9	−1.1	25.3	**−1.8%**		**FF8.5**	−28.4	30.3	97.0	**43.7%**
SO_2	16.10	**NF4.5**	−2.8	−0.3	2.4	**−1.7%**	19.29	**NF4.5**	−7.6	2.3	11.4	**11.8%**
		NF8.5	−2.0	0.3	2.6	**1.8%**		**NF8.5**	−7.3	1.6	10.0	**8.0%**
		FF4.5	−3.7	−1.1	2.7	**−6.9%**		**FF4.5**	−6.3	3.0	12.4	**15.7%**
		FF8.5	−4.7	−0.7	3.6	**−4.4%**		**FF8.5**	−4.8	7.8	22.0	**40.4%**

4.5 (RCP 8.5), respectively. SO_2 has also revealed notable increases, that the projected increases for RCP 4.5 (RCP 8.5) are 6.0% (4.0%) in near future, and 12.2% (15.2%) in the far future, respectively. The only relatively notable change in SON is found in the departure of O_3, with projected increases of 3.6% and 3.8% for RCP 4.5 and RCP 8.5 in near future, respectively, while those in far future are 7.2% and 13.0% for RCP 4.5 and RCP 8.5 respectively. Nonetheless, air pollutant concentrations are projected to decrease in JJA. The most notable result is the significant decreases in all pollutant concentrations in the far future, as of 4.6% (21.7%) for O_3, 1.0% (10.3%) for RSP, and 4.4% (22.4%) for SO_2 arranged by RCP 4.5 (RCP 8.5). The improving air quality is projected to occur in distant decades, as the changes in the near future are less significant in both scenarios.

After all, it can be concluded that direction of change varies in different seasons. Consistent increase is revealed in DJF and MAM, while the concentration tends to decrease in JJA. Among three pollutants, O_3 relatively shows the greater changes, especially in SON and MAM. The size of change depends a lot on the scenario, as it is found that projected changes under RCP 8.5 scenarios are significantly more severe than RCP 4.5 scenarios.

The projections cover a range of uncertainty. The minimum and maximum extreme values are included in the projections, showing that uncertainty ranges cover both signs for most of the projections. In spite of this, O_3 projection in MAM far future for both scenarios and SO_2 projection in MAM far future for RCP 8.5 have recorded a strict increase for all modal combination distributions, pointing to the conclusion that under certain scenarios, O_3 and SO_2 mean concentration in MAM will increase in far future.

To study the occurrence of high pollutant concentration in the future, the recent 95th percentile is calculated for each pollutant in each season from an average of the study sites. The 95th percentiles in recent years are defined as a threshold level to assess the changes in extreme air pollution in future climate scenarios, see Table 4. Consistent with the mean change in distribution, the occurrence percentages of extreme value show a similar pattern among seasons and scenarios. Concerning the mean distribution, distributions representing far future RCP 8.5 scenarios show more significant changes. Distributions in spring and winter show a significant increase, whereas JJA is projected to decrease in pollutant concentrations. Despite the model uncertainty concerned here, there still exists a tendency that extreme pollution cases will increase based on the prediction of the meteorological variable under the projected climate change. Particularly, some projections show a significant change even when all combinations of ensemble members in Monte Carlo calculations are taken into account (these distributions are marked with* in the table).

3.3. Discussion on contribution of the predictor variables on future variation of air quality

Figs. 2–4 demonstrate the contributions of meteorological variables to the future variation in pollutant concentration. The contribution values are defined by the multiplication of future mean deviation and

Table 4
Future occurrence percentage of recent 95th percentile (Q95) under different scenarios of different seasons. Q95 values are in μg/m^3, and others are in percentage (%). Minimum (Min), mean and maximum (Max) projection among all climate models are considered. Numbers highlighted in blue indicate negative changes (the occurrence percentage < 5%), while numbers highlighted in red indicate positive changes (the occurrence percentage > 5%). The darker the color, the stronger the correlation. Projections showing a consistent change among all combinations of climate models are marked with*. DJF refers to December–January–February; MAM refers to March–April–May; JJA refers to June–July–August; and SON refers to September-October-November.

	MAM					JJA					SON					DJF				
	Q95	Scenario	Min	Mean	Max	Q95	Scenario	Min	Mean	Max	Q95	Scenario	Min	Mean	Max	Q95	Scenario	Min	Mean	Max
O_3	48.99	NF4.5	1.9	6.6	20.6	32.26	NF4.5	3.3	4.3	5.8	54.21	NF4.5	2.5	5.3	11.2	42.68	NF4.5	4.5	5.8	8.8
		NF8.5	0.0	3.5	8.4		NF8.5	2.3	3.5	5.8		NF8.5	3.0	5.2	9.4		NF8.5	4.2	6.1	10.0
		FF4.5	3.0	8.0	17.9		FF4.5	2.5	3.9	6.0		FF4.5	4.2	5.7	7.9		FF4.5	4.0	6.1	11.0
		FF8.5	4.0	8.8	20.0		FF8.5	0.0*	1.8*	5.0*		FF8.5	3.6	6.7	19.0		FF8.5	4.5	9.4	21.2
RSP	46.37	NF4.5	0.0	3.8	6.2	27.40	NF4.5	2.9	4.8	8.2	57.47	NF4.5	0.0	4.3	7.6	67.33	NF4.5	3.7	6.7	7.6
		NF8.5	0.0	5.0	13.0		NF8.5	3.9	5.4	6.4		NF8.5	3.8	4.5	5.5		NF8.5	4.3	7.9	12.7
		FF4.5	0.0	5.6	11.4		FF4.5	3.9	4.8	6.7		FF4.5	3.1	5.0	6.8		FF4.5	0.0	5.8	12.7
		FF8.5	4.7	6.4	10.2		FF8.5	2.4*	3.1*	4.3*		FF8.5	0.0	5.1	7.5		FF8.5	3.9	9.5	19.3
SO_2	12.60	NF4.5	0.0	5.3	11.5	12.05	NF4.5	2.3	5.4	8.3	16.06	NF4.5	3.7	4.4	6.3	18.92	NF4.5	4.4	6.3	8.1
		NF8.5	0.0	5.3	13.6		NF8.5	3.5	5.3	8.2		NF8.5	4.2*	4.7*	4.8*		NF8.5	4.5	7.5	11.0
		FF4.5	3.3	7.3	15.7		FF4.5	3.4	5.1	7.1		FF4.5	2.7	4.0	7.4		FF4.5	2.5	6.4	11.0
		FF8.5	6.5*	9.2*	15.1*		FF8.5	0.0*	3.3*	5.0*		FF8.5	2.3	4.2	7.2		FF8.5	4.1	9.5	19.2

the GLM coefficients of each standardized meteorological variable. Herein, we highlight numerous notable contributions of the variables that have statistically significant deviation from the recent mean and have statistically significant correlation with pollutant concentration. We express these contributions in a percentage relative to the recent mean of pollutant concentration. Values in blanket indicate the exact contribution and the range of the 90% confidence interval.

The most significant contributions to the future variation are generally found under RCP 8.5 scenario in the far future. Among the contributions by various meteorological variables, it is found that in terms of magnitude, the contributions by surface temperature are the greatest in all seasons and for all pollutants, with a range from 56.9% to 65.2% relative to all contributions. These contributions, however, can be positive or negative. The significant elevation of far future surface temperature in JJA has contributed to the projected 36.66% (ac: 11.82 μg/m^3; cr: −12.83 to −10.26 μg/m^3), 12.84% (ac: −3.52 μg/m^3; cr: −3.82 to −3.05 μg/m^3) and 28.91% (ac: −3.48 μg/m^3; cr: −3.99 to −2.81 μg/m^3) decrease in O_3, RSP and SO_2 concentration, respectively. Surface temperature is also projected to reduce the RSP concentration at percentages of 22.15% (ac: −10.27 μg/m^3; cr: −14.13 to −5.55 μg/m^3) and 19.96% (ac: −11.47 μg/m^3; cr: −14.30 to −8.77 μg/m^3) in MAM and SON, respectively, and SO_2 concentration at percentages of 14.45% (ac: −2.32 μg/m^3; cr: −2.82 to −1.77 μg/m^3) in SON, respectively. Elevation of surface temperature tends to strengthen buoyancy force available to drive vertical mixing (Tong et al., 2018). Also, higher surface temperature is associated with weaker winter monsoon, a large-scale synoptic system which favours pollutant concentrations emitted from non-local inland source regions (Tong et al., 2018). Unlike JJA, surface temperature increase tends to enhance O_3 concentration in other seasons, and the contribution is relatively significant in DJF at a 12.87% (ac: 5.49 μg/m^3; 3.66–4.30 μg/m^3), possibly due to the principal role of temperature during O_3 formation

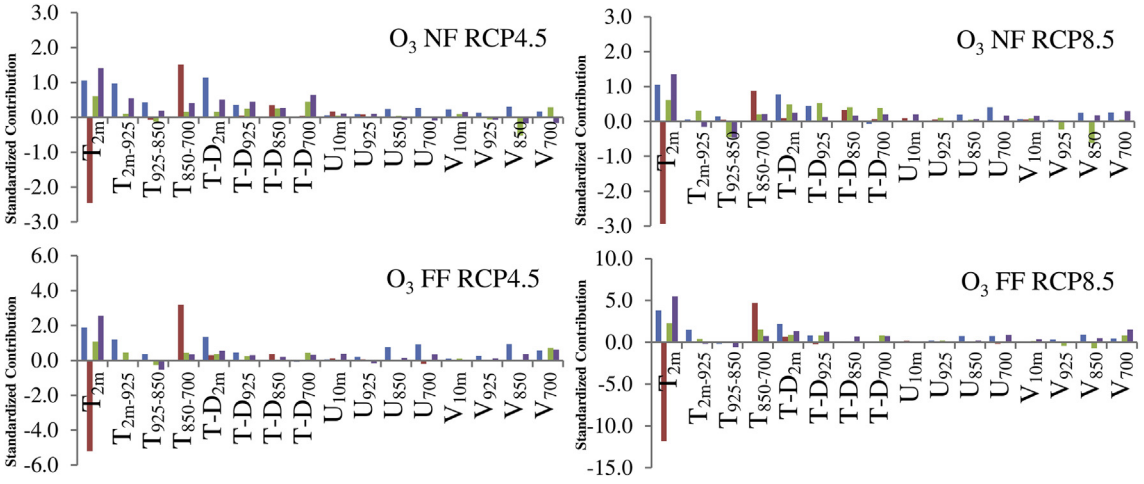

Fig. 2. Contribution of meteorological variables on the projected O_3 concentration based on different scenarios. The values are standardized by the recent mean and standard deviation. Bars in blue refers to March–April–May (MAM); red refers to June–July–August (JJA); green refers to September–October–November (SON); and purple refers to December–January–February (DJF). (For interpretation of the references to color in this figure legend, the reader is referred to the Web version of this article.)

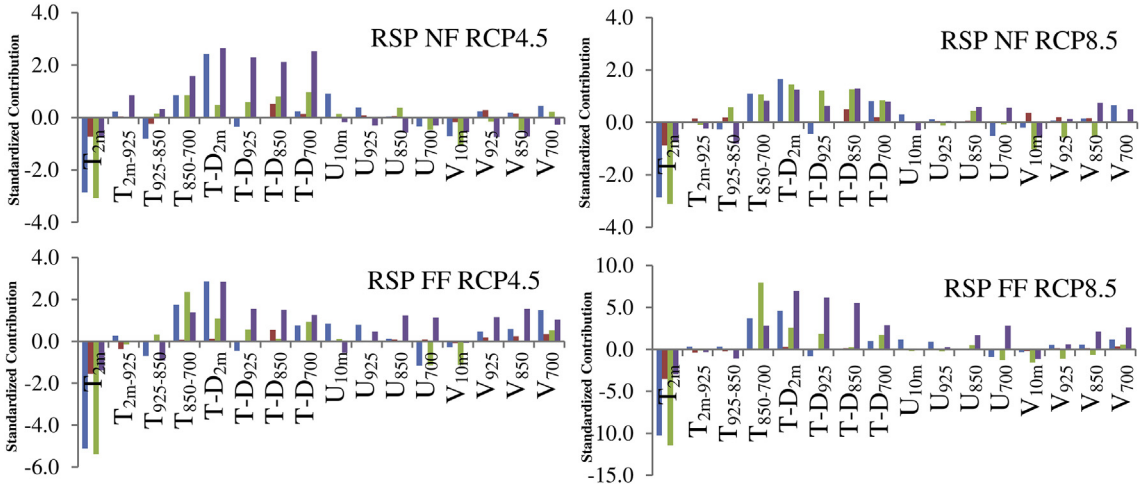

Fig. 3. Contribution of meteorological variables on the projected RSP concentration based on different scenarios. The values are standardized by the recent mean and standard deviation. Bars in blue refers to March–April–May (MAM); red refers to June–July–August (JJA); green refers to September–October–November (SON); and purple refers to December–January–February (DJF). (For interpretation of the references to color in this figure legend, the reader is referred to the Web version of this article.)

(Jacob and Winner, 2009; Rasmussen et al., 2012). Contribution in RCP 4.5 is relatively less significant, but we also obtain significant contributions including 16.16% (ac: −5.21 μg/m^3; cr: −7.21 to −4.08 μg/m^3) decreases to O_3 in JJA, 11.02% (ac: −5.11 μg/m^3; cr: −8.35 to −2.88 μg/m^3) decreases to RSP in MAM and 12.75% (ac: −1.54 μg/m^3; cr: −2.38 to −0.95 μg/m^3) decreases to SO_2 in JJA.

The projected positive contributions by surface temperature on RSP and SO_2 are partially offset by other variables. When considering the combined contributions grouped by variable natures, it is found that variables of temperature–dew point difference are projected to increase among all significant cases (Table 2), and these combined variables have contributed significantly to the future pollutant concentration deviations in numerous circumstances. For instance, these variables are projected to increase RSP concentration by 10.47% (ac: 4.85 μg/m^3; cr: −0.10–9.85 μg/m^3), 11.13% (ac: 6.39 μg/m^3; cr: −9.15–30.54 μg/m^3) and 32.05% (ac: 21.58 μg/m^3; cr: −0.38–70.51 μg/m^3) in MAM, SON and DJF, respectively, and increase SO_2 concentration by 26.95% (ac: 5.10 μg/m^3; cr: −0.05–16.60 μg/m^3) in DJF. We also note that even under the near future RCP 4.5 projection, combined temperature–dew point difference variables have also increase RSP and SO_2 concentration by 14.24% (ac: 9.58 μg/m^3; cr: −10.26–36.75 μg/m^3) and 12.06% (ac: 2.28 μg/m^3; cr: −2.41–8.72 μg/m^3) in DJF, respectively. The projected increase of temperature–dew point difference, literally indicating lower relative humidity may be associated with a weaker marine clear air (Tai et al., 2010), as well as less likelihood of precipitation and hence wet deposition (Chan and Kwok, 2001; Zhao et al., 2016). Both of these factors favour pollutant concentration. Within the group of the four variables representing different altitude, the contribution generally decreases with increasing altitude due to both greater sensitivity and more significant deviation at the surface in the future.

We also reveal the significantly positive contribution of 850 mb–700 mb temperature gradient ($T_{850\text{-}700}$) to O_3 and RSP in particular seasons. Projected reduction of the gradient in JJA is suggested to increase O_3 concentration by 14.5% (ac: 4.68 μg/m^3; cr: −4.59–9.68 μg/m^3), and that in SON is suggested to increase RSP concentration by 13.83% (ac: 7.95; cr: 5.41–12.08 μg/m^3). A smaller temperature gradient inhibits the vertical removal of surface air pollutants underneath the troposphere. Despite the general idea that the contribution and effect of meteorological variables attenuate along altitude, the result reveals that the contribution does not differ much

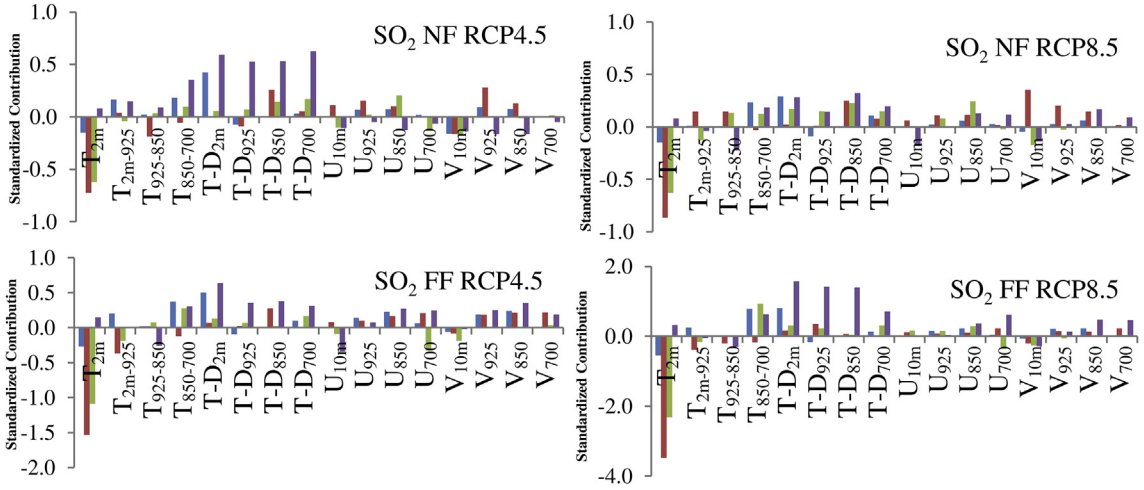

Fig. 4. Contribution of meteorological variables on the projected SO_2 concentration based on different scenarios. The values are standardized by the recent mean and standard deviation. Bars in blue refers to March–April–May (MAM); red refers to June–July–August (JJA); green refers to September–October–November (SON); and purple refers to December–January–February (DJF). (For interpretation of the references to color in this figure legend, the reader is referred to the Web version of this article.)

along different vertical levels. The contribution of middle tropospheric temperature difference (T_{850}-T_{700}) is observed even more significant than that of surface temperature difference (T_{2m}-T_{925}), possibly due to the greater association with the synoptic patterns. The contributions generated among the four scenarios differ mostly in the changes in magnitude, keeping the signs the same since the direction of meteorological variable changes is the same.

4. Conclusions

This study aims to statistically assess the impact of climate change alone on the future air quality in the Pearl River Delta region based on its current sensitivity to meteorological variables, and to analyse the contribution of several meteorological variables that reflect vertical atmospheric stability in altering the concentration of air pollutants in different seasons, under two studied emission scenarios (RCP 4.5 and RCP 8.5). Based on the ensemble of climate models, surface temperature is projected to increase significantly in all seasons. Significant increase in temperature–dew point difference is found in particular seasons and scenarios. There is also a projected significant deviation of vertical temperature gradient in certain situations.

Our projections show an increase in air pollutants, even though a decrease in air pollutants in JJA is projected. The changes are more significant in the far future, and under RCP 8.5 scenario. Despite that increase in future surface temperature is the critical factor to the future air quality change, changes in future vertical temperature gradient and the temperature–dew point difference are also projected to contribute to the increase in mean pollutant level. We also note the change in intensity and frequency of pollution conditions of all three pollutants under the two RCP scenarios. The probability of extreme air pollution episodes in future years is examined based on recent 95th percentile. The occurrence proportion of pollutant concentration greater than the recent 95th percentile is projected to be increased by 9.5%–9.6% in DJF, and 6.4%–9.2% in MAM.

To conclude, our results point to the notable potential effects of climate change, from the perspectives of vertical atmospheric conditions on air quality. Future air quality forecast should pay more attention on the climate change effect on the vertical profile of the atmosphere. Moreover, climate change alone is projected to have a remarkable effect on air quality in the PRD region in future, implying the necessity of more stringent future air quality emission control policies to mitigate air pollution in the future.

Acknowledgment

This work is jointly funded by the *Improvement on Competitiveness in Hiring New Faculties Fund* (2013/14) of The Chinese University of Hong Kong; The Vice-Chancellor's Discretionary Fund of The Chinese University of Hong Kong (grant no. 4930744) and the Early Career Scheme of Research Grants Council of Hong Kong (grant no. ECS-24301415). We would like to thank the Hong Kong Environmental Protection Department and the Hong Kong Observatory for providing air quality and meteorological data, respectively and the Information Technology Services Centre (ITSC) at CUHK for technical support. We also thank the two anonymous reviewers for their valuable comments and suggestions.

References

Baklanov, A., Rasmussen, A., Fay, B., Berge, E., Finardi, S., 2002. Potential and shortcomings of numerical weather prediction models in providing meteorological data for urban air pollution forecasting. Water Air Soil Pollut. Focus 2, 43–60.

Borge, R., Alexandrov, V., José del Vas, J., Lumbreras, J., Rodríguez, E., 2008. A comprehensive sensitivity analysis of the WRF model for air quality applications over the Iberian Peninsula. Atmos. Environ. 42, 8560–8574. https://doi.org/10.1016/j.atmosenv.2008.08.032.

Chan, L., Kwok, W.S., 2001. Roadside suspended particulates at heavily trafficked urban sites of Hong Kong – seasonal variation and dependence on meteorological conditions. Atmos. Environ. 35, 3177–3182. https://doi.org/10.1016/S1352-2310 (00) 00504-5.

Che, W., Zheng, J., Wang, S., Zhong, L., Lau, A., 2011. Assessment of motor vehicle emission control policies using Model-3/CMAQ model for the Pearl River Delta region, China. Atmos. Environ. 45, 1740–1751. https://doi.org/10.1016/j.atmosenv.2010.12.050.

Chylek, P., Li, J., Dubey, M.K., Wang, M., Lesins, G., 2011. Observed and model simulated 20th century arctic temperature variability: canadian earth system model CanESM2. Atmos. Chem. Phys. Discuss. 11, 22893–22907. https://doi.org/10.5194/acpd-11-22893-2011.

Collins, W.J., 2003. Effect of stratosphere-troposphere exchange on the future tropospheric ozone trend. J. Geophys. Res. 108. https://doi.org/10.1029/2002JD002617.

Dawson, J.P., Adams, P.J., Pandis, S.N., 2007. Sensitivity of ozone to summertime climate in the eastern USA: a modeling case study. Atmos. Environ. 41, 1494–1511. https://doi.org/10.1016/j.atmosenv.2006.10.033.

Fiore, A.M., Dentener, F.J., Wild, O., Cuvelier, C., Schultz, M.G., Hess, P., Textor, C., Schulz, M., Doherty, R.M., Horowitz, L.W., MacKenzie, I.A., Sanderson, M.G., Shindell, D.T., Stevenson, D.S., Szopa, S., Van Dingenen, R., Zeng, G., Atherton, C., Bergmann, D., Bey, I., Carmichael, G., Collins, W.J., Duncan, B.N., Faluvegi, G., Folberth, G., Gauss, M., Gong, S., Hauglustaine, D., Holloway, T., Isaksen, I.S.A., Jacob, D.J., Jonson, J.E., Kaminski, J.W., Keating, T.J., Lupu, A., Marmer, E., Montanaro, V., Park, R.J., Pitari, G., Pringle, K.J., Pyle, J.A., Schroeder, S., Vivanco, M.G., Wind, P., Wojcik, G., Wu, S., Zuber, A., 2009. Multimodel estimates of intercontinental source-receptor relationships for ozone pollution. J. Geophys. Res. 114. https://doi.org/10.1029/2008JD010816.

Fiore, A.M., Naik, V., Spracklen, D.V., Steiner, A., Unger, N., Prather, M., Bergmann, D., Cameron-Smith, P.J., Cionni, I., Collins, W.J., Dalsøren, S., Eyring, V., Folberth, G.A., Ginoux, P., Horowitz, L.W., Josse, B., Lamarque, J.-F., MacKenzie, I.A., Nagashima, T., O'Connor, F.M., Righi, M., Rumbold, S.T., Shindell, D.T., Skeie, R.B., Sudo, K., Szopa, S., Takemura, T., Zeng, G., 2012. Global air quality and climate. Chem. Soc. Rev. 41, 6663. https://doi.org/10.1039/c2cs35095e.

George, J.J., 1960. Weather Forecasting for Aeronautics. New York and London Academic Press.

Ginn, W.L., Lee, T.C., Chan, K.Y., 2010. Past and future changes in the climate of Hong Kong. J. Meteorol. Res. 24, 163–175.

Giorgetta, M.A., Jungclaus, J., Reick, C.H., Legutke, S., Bader, J., Böttinger, M., Brovkin, V., Crueger, T., Esch, M., Fieg, K., Glushak, K., Gayler, V., Haak, H., Hollweg, H.-D., Ilyina, T., Kinne, S., Kornblueh, L., Matei, D., Mauritsen, T., Mikolajewicz, U., Mueller, W., Notz, D., Pithan, F., Raddatz, T., Rast, S., Redler, R., Roeckner, E., Schmidt, H., Schnur, R., Segschneider, J., Six, K.D., Stockhause, M., Timmreck, C., Wegner, J., Widmann, H., Wieners, K.-H., Claussen, M., Marotzke, J., Stevens, B., 2013. Climate and carbon cycle changes from 1850 to 2100 in MPI-ESM simulations for the coupled model intercomparison project phase 5: climate changes in MPI-ESM. J. Adv. Model. Earth Syst. 5, 572–597. https://doi.org/10.1002/jame.20038.

Gu, Y., Yim, S.H.L., 2016. The air quality and health impacts of domestic trans-boundary pollution in various regions of China. Environ. Int. 97, 117–124. https://doi.org/10.1016/j.envint.2016.08.004.

Hedegaard, G.B., Brandt, J., Christensen, J.H., Frohn, L.M., Geels, C., Hansen, K.M., Stendel, M., 2008. Impacts of climate change on air pollution levels in the northern hemisphere with special focus on Europe and the arctic. In: Borrego, C., Miranda, A.I. (Eds.), Air Pollution Modeling and its Application XIX. Springer Netherlands, Dordrecht, pp. 568–576. https://doi.org/10.1007/978-1-4020-8453-9_62.

Hogrefe, C., Lynn, B., Civerolo, K., Ku, J.-Y., Rosenthal, J., Rosenzweig, C., Goldberg, R., Gaffin, S., Knowlton, K., Kinney, P.L., 2004. Simulating changes in regional air pollution over the eastern United States due to changes in global and regional climate and emissions. J. Geophys. Res. Atmos. 109, D22301. https://doi.org/10.1029/2004JD004690.

Huang, J.P., Fung, J.C., Lau, A.K., Qin, Y., 2005. Numerical simulation and process analysis of typhoon-related ozone episodes in Hong Kong. J. Geophys. Res. Atmosphere 110, D05301. https://doi.org/10.1029/2004JD004914.

Hulme, M., 2002. Tyndall Centre for climate change research. In: Climate Change Scenarios for the United Kingdom: the UKCIP02 Scientific Report. Tyndall Centre for Climate Change Research, School of Environmental Sciences, University of East Anglia, Norwich, UK.

IPCC, 2014. Climate change. In: In: Pachauri, R.K., Meyer, L.A. (Eds.), Synthesis Report. Contribution of 505 Working Groups I, II and III to the Fifth Assessment Report of the Intergovernmental Panel on Climate Change, vol. 506. pp. 1e151 Geneva, Switzerland, 2014.

Jacob, D.J., Winner, D.A., 2009. Effect of climate change on air quality. Atmos. Environ. 43, 51–63. https://doi.org/10.1016/j.atmosenv.2008.09.051.

Jiang, D., Tian, Z., Lang, X., 2016. Reliability of climate models for China through the IPCC third to fifth assessment reports: reliability of climate models for China. Int. J. Climatol. 36, 1114–1133. https://doi.org/10.1002/joc.4406.

Krüger, B.C., Katragkou, E., Tegoulias, I., Zanis, P., Melas, D., Coppola, E., Rauscher, S., Huszar, P., Halenka, T., 2008. Regional photochemical model calculations for Europe concerning ozone levels in a changing climate. Idojaras 112, 285–300.

Lee, T., Chan, K., Ginn, W., 2011. Projection of extreme temperatures in Hong Kong in the 21st century. Acta Meteorol. Sin. 25, 1–20. https://doi.org/10.1007/s13351-011-0001-3.

Leung, L.R., Gustafson Jr., W.I., 2005. Potential regional climate change and implications to U.S. air quality. Geophys. Res. Lett. 32. https://doi.org/10.1029/2005GL022911.

Lin, C.Y., Chua, Y.J., Sheng, Y.F., Hsu, H.H., Cheng, C.T., Lin, Y.Y., 2015. Altitudinal and latitudinal dependence of future warming in Taiwan simulated by WRF nested with ECHAM5/MPIOM: future warming in an island of multi climate zones. Int. J. Climatol. 35, 1800–1809. https://doi.org/10.1002/joc.4118.

Lin, J.T., Patten, K.O., Hayhoe, K., Liang, X.Z., Wuebbles, D.J., 2008. Effects of future climate and biogenic emissions changes on surface ozone over the United States and China. J. Appl. Meteorol. Climatol. 47, 1888–1909. https://doi.org/10.1175/2007JAMC1681.1.

Liu, Q., Lam, K.S., Jiang, F., Wang, T.J., Xie, M., Zhuang, B.L., Jiang, X.Y., 2013. A numerical study of the impact of climate and emission changes on surface ozone over South China in autumn time in 2000–2050. Atmos. Environ. 76, 227–237. https://doi.org/10.1016/j.atmosenv.2013.01.030.

Lo, J.C.F., Lau, A.K.H., Fung, J.C.H., Chen, F., 2006. Investigation of enhanced cross-city transport and trapping of air pollutants by coastal and urban land-sea breeze circulations. J. Geophys. Res. 111. https://doi.org/10.1029/2005JD006837.

Luo, M., Hou, X., Gu, Y., Lau, N.C., Yim, S.H.L., 2018. Trans-boundary air pollution in a city under various atmospheric conditions. Sci. Total Environ. 618, 132–141. https://doi.org/10.1016/j.scitotenv.2017.11.001.

Mickley, L.J., 2004. Effects of future climate change on regional air pollution episodes in the United States. Geophys. Res. Lett. 31. https://doi.org/10.1029/2004GL021216.

Miller, R.C., 1967. Notes on Analysis and Severe-storm Forecasting Procedures of the Military Weather Warning Center. Air Weather Service (MAC). United States Air Force.

Morris, R.E., Gery, M.S., Liu, M.K., Moore, G.E., Daly, C., Greenfield, S.M., 1989. Sensitivity of a regional oxidant model to variations in climate parameters. In: Smith, J.B., Tirpak, D.A. (Eds.), The Potential Effects of Global Climate Change on the United States. USEPA, Office of Policy, Planning and Evaluation, Washington, DC, USA.

Morris, R.E., Guthrie, P.D., Knopes, C.A., 1995. Photochemical analysis under global warming conditions. In: Proceedings of the 88th Air and Waste Management Association Annual Meeting, June 18-23, 1995, San Antonio, Texas. Air and Waste Management Association, Pittsburgh, PA, USA.

Murazaki, K., Hess, P., 2006. How does climate change contribute to surface ozone change over the United States? J. Geophys. Res. 111. https://doi.org/10.1029/2005JD005873.

Penner, J.E., Connell, P.S., Wuebbles, D.J., Covey, C.C., 1989. Climate change and its interaction with air chemistry: perspectives and research needs. In: Smith, J.B., Tirpak, D.A. (Eds.), The Potential Effects of Global Climate Change on the United States, Appendix F: Air Quality. EPA-230- 05-89-056. Environmental Protection Agency, Washington, DC, USA.

Pielke Sr., R.A., Avissar, R., Raupach, M., Dolman, A.J., Zeng, X., Denning, A.S., 1998. Interactions between the atmosphere and terrestrial ecosystems: influence on weather and climate. Global Change Biol. 4, 461–475. https://doi.org/10.1046/j.1365-2486.1998.t01-1-00176.x.

Rasmussen, D.J., Fiore, A.M., Naik, V., Horowitz, L.W., McGinnis, S.J., Schultz, M.G., 2012. Surface ozone-temperature relationships in the eastern US: a monthly climatology for evaluating chemistry-climate models. Atmos. Environ. 47, 142–153. https://doi.org/10.1016/j.atmosenv.2011.11.021.

Shir, C.C., Shieh, L.J., 1974. A generalized urban air pollution model and its application to the study of SO 2 distributions in the st. Louis metropolitan area. J. Appl. Meteorol. 13, 185–204. https://doi.org/10.1175/1520-0450-13.2.185.

Sillman, S., 1999. The relation between ozone, NOx and hydrocarbons in urban and polluted rural environments. Atmos. Environ. 33, 1821–1845. https://doi.org/10.1016/S1352-2310(98)00345-8.

Sillman, S., Samson, P.J., 1995. Impact of temperature on oxidant photochemistry in urban, polluted rural and remote environments. J. Geophys. Res. 100, 11497. https://doi.org/10.1029/94JD02146.

Stevenson, D.S., Dentener, F.J., Schultz, M.G., Ellingsen, K., van Noije, T.P.C., Wild, O., Zeng, G., Amann, M., Atherton, C.S., Bell, N., Bergmann, D.J., Bey, I., Butler, T., Cofala, J., Collins, W.J., Derwent, R.G., Doherty, R.M., Drevet, J., Eskes, H.J., Fiore, A.M., Gauss, M., Hauglustaine, D.A., Horowitz, L.W., Isaksen, I.S.A., Krol, M.C., Lamarque, J.-F., Lawrence, M.G., Montanaro, V., Müller, J.-F., Pitari, G., Prather, M.J., Pyle, J.A., Rast, S., Rodriguez, J.M., Sanderson, M.G., Savage, N.H., Shindell, D.T., Strahan, S.E., Sudo, K., Szopa, S., 2006. Multimodel ensemble simulations of present-day and near-future tropospheric ozone. J. Geophys. Res. 111. https://doi.org/10.1029/2005JD006338.

Tagaris, E., Manomaiphiboon, K., Liao, K.-J., Leung, L.R., Woo, J.-H., He, S., Amar, P., Russell, A.G., 2007. Impacts of global climate change and emissions on regional ozone and fine particulate matter concentrations over the United States. J. Geophys. Res. 112. https://doi.org/10.1029/2006JD008262.

Tai, A.P., Mickley, L.J., Jacob, D.J., 2010. Correlations between fine particulate matter (PM2.5) and meteorological variables in the United States: implications for the sensitivity of PM2.5 to climate change. Atmos. Environ. 44, 3976–3984. https://doi.org/10.1016/j.atmosenv.2010.06.060.

Tong, C.H.M., Yim, S.H.L., Rothenberg, D., Wang, C., Lin, C.-Y., Chen, Y.D., Lau, N.C., 2018. Assessing the impacts of seasonal and vertical atmospheric conditions on air quality over the Pearl River Delta region. Atmos. Environ. 180, 69–78. https://doi.org/10.1016/j.atmosenv.2018.02.039.

Wang, T., 2003. Characterizing the temporal variability and emission patterns of pollution plumes in the Pearl River Delta of China. Atmos. Environ. 37, 3539–3550. https://doi.org/10.1016/S1352-2310(03)00363-7.

Wang, X., Chen, F., Wu, Z., Zhang, M., Tewari, M., Guenther, A., Wiedinmyer, C., 2009. Impacts of weather conditions modified by urban expansion on surface ozone: comparison between the Pearl River Delta and Yangtze River Delta regions. Adv. Atmos. Sci. 26, 962–972. https://doi.org/10.1007/s00376-009-8001-2.

Wang, X., Liao, J., Zhang, J., Shen, C., Chen, W., Xia, B., Wang, T., 2014. A numeric study of regional climate change induced by urban expansion in the Pearl River Delta, China. J. Appl. Meteorol. Climatol. 53, 346–362. https://doi.org/10.1175/JAMC-D-13-054.1.

Wang, X.-K., Lu, W.-Z., 2006. Seasonal variation of air pollution index: Hong Kong case study. Chemosphere 63, 1261–1272. https://doi.org/10.1016/j.chemosphere.2005.10.031.

Watanabe, M., Suzuki, T., O'ishi, R., Komuro, Y., Watanabe, S., Emori, S., Takemura, T., Chikira, M., Ogura, T., Sekiguchi, M., Takata, K., Yamazaki, D., Yokohata, T., Nozawa, T., Hasumi, H., Tatebe, H., Kimoto, M., 2010. Improved climate simulation by MIROC5: mean states, variability, and climate sensitivity. J. Clim. 23, 6312–6335. https://doi.org/10.1175/2010JCLI3679.1.

Willmott, C.J., Robeson, S.M., Matsuura, K., 2012. A refined index of model performance. Int. J. Climatol. 32, 2088–2094. https://doi.org/10.1002/joc.2419.

Wong, T.W., Tam, W.W.S., Yu, I.T.S., Lau, A.K.H., Pang, S.W., Wong, A.H.S., 2013. Developing a risk-based air quality health index. Atmos. Environ. 76, 52–58. https://doi.org/10.1016/j.atmosenv.2012.06.071.

Wu, D., Tie, X., Li, C., Ying, Z., Kai-Hon Lau, A., Huang, J., Deng, X., Bi, X., 2005. An extremely low visibility event over the Guangzhou region: a case study. Atmos. Environ. 39, 6568–6577. https://doi.org/10.1016/j.atmosenv.2005.07.061.

Wu, S., Mickley, L.J., Leibensperger, E.M., Jacob, D.J., Rind, D., Streets, D.G., 2008. Effects of 2000–2050 global change on ozone air quality in the United States. J. Geophys. Res. 113. https://doi.org/10.1029/2007JD008917.

Yim, S.H.L., Fung, J.C.H., Lau, A.K.H., Kot, S.C., 2007. Developing a high-resolution wind map for a complex terrain with a coupled MM5/CALMET system. J. Geophys. Res. 112, D05106. https://doi:10.1029/2006JD007752.

Yim, S.H.L., Fung, J.C.H., Lau, A.K.H., 2010. Use of high-resolution MM5/CALMET/CALPUFF system: SO2 apportionment to air quality in Hong Kong. Atmos. Environ. 44 (38), 4850–4858. https://doi.org/10.1016/j.atmosenv.2010.08.037.

Yukimoto, S., Adachi, Y., Hosaka, M., Sakami, T., Yoshimura, H., Hirabara, M., Tanaka, T.Y., Shindo, E., Tsujino, H., Deushi, M., Mizuta, R., Yabu, S., Obata, A., Nakano, H., Koshiro, T., Ose, T., Kitoh, A., 2012. A New global climate model of the meteorological research institute: MRI-CGCM3 —model description and basic performance—. J. Meteorol. Soc. Jpn. 90A, 23–64. https://doi.org/10.2151/jmsj.2012-A02.

Zhang, Y.H., Hu, M., Zhong, L.J., Wiedensohler, A., Liu, S.C., Andreae, M.O., Wang, W., Fan, S.J., 2008a. Regional integrated experiments on air quality over Pearl River Delta 2004 (PRIDE-PRD2004): overview. Atmos. Environ. 42, 6157–6173. https://doi.org/10.1016/j.atmosenv.2008.03.025.

Zhang, Y.H., Su, H., Zhong, L.J., Cheng, Y.F., Zeng, L.M., Wang, X.S., Xiang, Y.R., Wang, J.L., Gao, D.F., Shao, M., 2008b. Regional ozone pollution and observation-based approach for analyzing ozone–precursor relationship during the PRIDE-PRD2004 campaign. Atmos. Environ. 42, 6203–6218. https://doi.org/10.1016/j.atmosenv.2008.05.002.

Zhao, W., Fan, S., Guo, H., Gao, B., Sun, J., Chen, L., 2016. Assessing the impact of local meteorological variables on surface ozone in Hong Kong during 2000–2015 using quantile and multiple line regression models. Atmos. Environ. 144, 182–193. https://doi.org/10.1016/j.atmosenv.2016.08.077.

Zheng, J., Zhang, L., Che, W., Zheng, Z., Yin, S., 2009. A highly resolved temporal and spatial air pollutant emission inventory for the Pearl River Delta region, China and its uncertainty assessment. Atmos. Environ. 43, 5112–5122. https://doi.org/10.1016/j.atmosenv.2009.04.060.